Temporal expectation hastens sensory encoding but does not affect evidence quality

Ruud L. van den Brink[1,2,*], Peter R. Murphy[1,2], Kobe Desender[1,3], Nicole de Ru[2], & Sander Nieuwenhuis[2,4]

[1]Department of Neurophysiology and Pathophysiology, University Medical Center Hamburg-Eppendorf, Hamburg, Germany
[2]Department of Psychology, Leiden University, Leiden, the Netherlands
[3]Department of Experimental Psychology, Ghent University, Belgium
[4]Leiden institute for Brain and Cognition, Leiden, the Netherlands
*To whom correspondence should be addressed: r.van-den-brink@uke.de

ABSTRACT

The ability to predict the timing of forthcoming events, known as temporal expectation, has a strong impact on human information processing. Although there is growing consensus that temporal expectations enhance perception, it remains unclear whether they affect the decision process itself, or non-decisional (sensory / motor) processes. Here, participants used predictive auditory cues to anticipate the timing of low-contrast visual imperative stimuli. Modelling of the behavioral data indicated that temporal expectations speeded up non-decisional processes but had no effect on decision formation. Electrophysiological recordings confirmed and extended this result: temporal expectations hastened the onset of a neural signature of decision formation, consistent with faster sensory encoding, but had no effect on its build-up rate. Anticipatory alpha-band power was modulated by temporal expectation, and co-varied with intrinsic trial-by-trial variability in behavioral and neural signatures of sensory encoding speed. These findings highlight how temporal predictions optimize our interaction with unfolding sensory events.

ACKNOWLEDGEMENTS

We thank Konstantinos Tsetsos for helpful comments on an earlier version of this article. This work was supported by a fellowship for postdoctoral researchers funded by the Alexander von Humboldt Foundation (to RLvdB), funding from the German Research Foundation (DFG; grant numbers DO 1240/3-1, DO 1240/4-1, and SFB 936/A7, to PM), an FWO [PEGASUS]² Marie Skłodowska-Curie fellowship (12T9717N, to KD), and a Consolidator Grant of the European Research Council (grant number GA 283314-NOREPI, to SN).

INTRODUCTION

To efficiently process the large amount of sensory information that we constantly receive, the brain actively predicts upcoming sensory input rather than passively registering it. One way the brain achieves this is by exploiting temporal contingencies in the continuous stream of sensory input. These contingencies can be used to prepare for relevant events and optimize processing of those events. The temporal expectations shaped by these contingencies have a profound impact on perception and action, enhancing the speed and, in some cases, the accuracy of responding in a wide range of information-processing tasks (Hackley & Valle-Inclán, 2003; Niemi & Näätänen, 1981; Nobre, Correa, & Coull, 2007; Nobre & van Ede, 2018). Recent research has established that the brain expresses such temporal expectations by synchronizing oscillatory neural dynamics (power and phase) with the temporal structure of the environment (Busch, Dubois, & VanRullen, 2009; Cravo, Rohenkohl, Wyart, & Nobre, 2013; Henry, Herrmann, & Obleser, 2014; Schroeder & Lakatos, 2009; Stefanics et al., 2010; van den Brink, Wynn, & Nieuwenhuis, 2014). For example, fluctuations in the amplitude of ongoing neural oscillations in the α band (9-12 Hz) closely track the time course of temporal expectations (Ergenoglu et al., 2004; Rohenkohl & Nobre, 2011; Thut, Nietzel, Brandt, & Pascual-Leone, 2006). In contrast, the mechanisms through which temporal expectations enhance task performance remain unclear. The goal of the current study was to identify how temporal expectations shape perception.

Although there is a growing consensus that temporal expectations enhance perception (Correa, Lupiáñez, Madrid, & Tudela, 2006; Correa, Lupiáñez, & Tudela, 2005; Jepma, Wagenmakers, & Nieuwenhuis, 2012; Rohenkohl, Cravo, Wyart, & Nobre, 2012a; Rolke & Hofmann, 2007; Vangkilde, Coull, & Bundesen, 2012), different studies have arrived at different conclusions as to whether this is achieved through (1) expedited encoding of the sensory evidence (Bausenhart, Rolke, Seibold, & Ulrich, 2010; Jepma et al., 2012; Seibold, Bausenhart, Rolke, & Ulrich, 2011), or (2) an increase in the *quality* of the sensory evidence. Under most computational frameworks for decision-making, the latter is equivalent to the mean rate at which evidence is accumulated (i.e., decision formation; Rohenkohl et al., 2012a; Vangkilde et al., 2012). One way to address this discrepancy is by decomposing performance on cognitive tasks into latent information-processing parameters using sequential-sampling models (Forstmann, Ratcliff, & Wagenmakers, 2016), and examining the effects of temporal expectations on those parameters. Previous attempts to discriminate between the sensory encoding account and evidence quality account employed such model-based analyses of behavioral data. However, recent studies on perceptual decision-making have revealed that conclusions based on prominent sequential-sampling models can be falsified by complementary analyses of neural signatures of decision formation (McGovern, Hayes, Kelly, & O'Connell, 2018; Spieser, Kohl, Forster, Bestmann, & Yarrow, 2018), suggesting that it is critical to corroborate insights from modelling with neural evidence. Specifically, non-invasive human EEG recordings have identified a domain-general build-to-threshold signal, the centroparietal positivity (CPP), that reflects decision formation via the gradual accumulation of sensory evidence (O'Connell, Shadlen, Wong-Lin, & Kelly, 2018). Neurophysiological findings indicate that the onset of the evidence accumulation process considerably lags initial sensory evidence encoding (Gold & Shaldlen, 2007; Huk & Shadlen 2005; Teichert, Grinband, & Ferrera, 2016), suggesting that measures of CPP onset latency and slope can be used to dissociate the speed of sensory evidence encoding from other influences on the decision process (evidence strength and the rate of accumulation), respectively (Loughnane et al., 2016).

To address the outstanding discrepancy in the literature, we combined these modelling and electrophysiological approaches to examine the effects of temporal expectations on perceptual decision-making in a temporal cuing task, a powerful paradigm for manipulating temporal expectations (Coull & Nobre, 1998). The two approaches provided strong, converging evidence for an account in which temporal expectations enhance task performance specifically by shortening the time needed for sensory encoding, and not by affecting the decision process (other than its onset). In addition, time–frequency analysis of the EEG data identified peri-stimulus α-band power as a significant factor underlying the effect of temporal expectation on sensory encoding.

MATERIALS AND METHODS

Participants. A total of 30 participants took part in the study. After EEG artifact rejection and predetermined exclusion criteria (see below), a total of 21 participants remained (mean age 22.6 years old; SD 2.4; range 18-28; 18 female). All participants had normal or corrected-to-normal vision, and were free from any neurological or psychiatric disorders. Participants gave written informed consent and were compensated with €7.50 or course credit. The experiment was approved by the Leiden University Institute of Psychology Ethics Committee.

Task. The task consisted of the detection of the appearance of a small opening (decrease in luminance, 0.19° by 0.23° visual angle) on either side of a white square box (side length = 2.34° visual angle) presented on a black background (Figure 1a). Participants reported the onset of the target stimulus (i.e., the small opening) by pressing the space bar of a computer keyboard with the index finger of their right hand, regardless of whether the target appeared on the left or the right. The target remained on the screen for one second, after which both the target and the surrounding box disappeared briefly (50 ms) to signal the onset of a new trial. If the participant responded after this time, the trial was counted as an error. If the participant responded before target onset, the text "You responded too soon!" appeared in red and the trial was aborted. Task difficulty was manipulated by adjusting the luminance of the target stimulus. The decrease in luminance relative to the surrounding box of easy and difficult targets (28% and 20%) was determined in a pilot experiment (N = 6), and set such that its effect on response time (RT) was of approximately the same size as the effect of cue validity on RT for the short cue-target interval (CTI; see below). This allowed a fair dissociation between underlying model parameters and electrophysiological markers.

In order to manipulate temporal expectation about target onset, we used the temporal cueing paradigm (Coull & Nobre, 1998). Following a 1.5 s fixation interval, target onset was probabilistically cued by a brief (150 ms) auditory signal. Cue 1 (440 Hz) signaled that the target would likely appear after 2700 ms (long CTI), and cue 2 (1320 Hz) signaled that the target would likely appear after 1350 ms (short CTI). The CTIs were chosen based on prior work (Stefanics et al., 2010). Both cues had a validity of 80%, such that on 20% of the trials the target would appear after the uncued interval (invalid trials). The cues and the target were presented in different sensory modalities so that participants could optimally distinguish them. The cue was presented in the auditory domain to ensure that participants perceived the cue even when briefly losing fixation.

As is common in the temporal cueing literature, we included a small proportion (13%) of catch trials, on which no target appeared after the cue. This ensures that participants generally await target presentation at the long CTI and make few anticipatory responses (Correa et al., 2006). These trials, along with a small amount of trials (mean = 4.0 s, SD = 5.1) on which participants responded before target onset, were excluded from all analyses.

Participants were instructed to maintain fixation throughout the task, to use the cue to speed up target detection, and to "respond as quickly and accurately as possible". In total, participants performed 8 blocks of 115 trials per block (920 in total). Participants briefly practiced the task beforehand (2 blocks of 24 trials). The total duration of the task was approximately 1 hour.

Behavioral data analysis. Effects of cue validity, CTI, and difficulty on RT and accuracy were tested with a repeated-measures ANOVA in JASP version 0.9.2 (JASP Team, 2018), with cue validity (valid or invalid), CTI (short or long), and difficulty (easy or difficult) as within-participant factors. Planned paired-samples t tests were conducted to examine the effect of cue validity on RT for the short CTI, the effect of difficulty on RT, and differences in the size of these two effects. Because we expected the effect of cue validity for the short CTI to be approximately the same size as the effect of difficulty, we calculated a Bayes factor (using default priors) for this statistical comparison in order to estimate the evidence for the null hypothesis of no difference. Bayes factors between zero and one indicate evidence for the null hypothesis, with $1/10 \leq BF \leq 1/3$ indicating "substantial" evidence for the null hypothesis (Wetzels & Wagenmakers, 2012).

Hierarchical drift diffusion modeling. We decomposed behavioral data from the target-detection task into latent parameters of the decision process using the drift diffusion model (DDM), a popular instance of sequential-sampling models of RT tasks (Forstmann, Ratcliff, & Wagenmakers, 2016; Ratcliff & McKoon, 2008). The DDM assumes that for two-alternative forced choice decisions, noisy sensory evidence is accumulated from a starting point z, at drift rate v, toward one of two decision bounds (thresholds), labeled 0 and a. When the accumulated evidence reaches one of the two bounds, the corresponding decision is initiated. The distance between the bounds, referred to as boundary separation, is equal to a. The model ascribes all non-decisional processes, including sensory encoding and response execution, to a non-decision time parameter T_{er}.

Most decision-making tasks require selecting between two overt responses. However, our task is similar to a go/no-go task, in that the participants have to arbitrate between a simple go decision when the target is presented and a no-go decision when the target is not presented. As a consequence, RTs for a no-go decision cannot be empirically measured. Therefore, in line with previous studies (e.g., Gomez, Ratcliff, & Perea, 2007; Zhang et al., 2016), we assumed an implicit lower decision bound for no-go decisions and an explicit upper boundary for go decisions. We then fitted the DDM to participants' decisions (i.e., the proportion of go and no-go decisions) as well as the distributions of RTs (for regular trials with correctly timed responses and for catch trials with commission errors).

We fitted this DDM to behavioral data (choices and RTs), using the hierarchical Bayesian model fitting procedure implemented in the HDDM toolbox (version 0.6.1; Wiecki, Sofer, & Frank, 2013). The HDDM uses Markov-chain Monte Carlo sampling, which generates full posterior distributions over parameter estimates, quantifying not only the most likely parameter value but also uncertainty associated with each estimate. Due to the hierarchical nature of the HDDM, estimates for individual participants are constrained by group-level prior distributions. In practice, this results in more stable estimates for individual participants, especially when working with low trial numbers (Vandekerckhove, Tuerlinckx, & Lee, 2011; Wiecki et al., 2013).

For each model fit, we drew 100,000 samples from the posterior distribution. The first 10% of these were discarded as burn-in and every second sample was discarded for thinning, reducing autocorrelation in the chains. Group-level chains were visually inspected to ensure convergence, ruling out sudden jumps in the posterior and ruling out autocorrelation. Additionally, the model that is reported in the main text was run three times in order to compute Gelman-Rubin $\hat{R}$ statistics (comparing within-chain and between-chain variance). We checked and confirmed that all group-level parameters had an $\hat{R}$ value between 0.98-1.02, suggesting convergence between these three instantiations of the same model. Because individual parameter estimates are constrained by group-level priors, data are not independent and therefore frequentist statistics cannot be used. The probability that a condition differs from another can be computed by calculating the overlap in posterior distributions. The fits of models of different complexity were compared to each other by calculating the deviance information criterion (DIC; Spiegelhalter, Best, Carlin, & van der Linde, 2002). Lower DIC values indicate that a model explains the data better, while taking model complexity into account. DIC differences larger than 10 are generally taken as strong evidence for a difference in model goodness-of-fit.

In the main text, we focus on a model in which both drift rate and non-decision time were free to vary as a function of cue validity, and drift rate was also free to vary as a function of difficulty. Apart from this model, we fitted and compared a variety of different models in which drift rate was always allowed to vary as a function of difficulty, and in which all possible combinations of drift rate, non-decision time and/or boundary separation were allowed to vary as a function of cue validity (Table 1). All models assumed an unbiased starting point ($z = a/2$). Cue validity was expected to reliably influence behavior for early, but not late targets (Correa et al., 2006). The lack of an effect for the long CTI is caused by the fact that on invalidly cued long-CTI trials, the participant can reorient temporal attention from the expected short CTI to the actual long CTI, in time for the target to appear. For this reason, we only fitted the behavioral data from trials with a short CTI. Trials on which participants failed to respond (i.e., misses, mean = 24.4 trials, SD 18.1) were considered trials on which the no-go bound was crossed. For these types of trials, RTs were set to NaN (i.e., not a number), so that the (missing)

RT did not contribute to the parameter estimation (as implemented in HDDM version 0.6.1), whereas the (erroneous) decision itself did contribute, thus facilitating accurate and reliable estimates of model parameters.

EEG recording and preprocessing. EEG data were recorded using a BioSemi ActiveTwo system from 64 channels placed according to the international 10/20 system. Additionally, a reference electrode was placed on each mastoid, and bipolar electro-oculogram (EOG) recordings were obtained from electrodes placed approximately 1 cm lateral of the outer canthi (horizontal EOG) and from electrodes placed approximately 1 cm above and below the left eye (vertical EOG). During acquisition, impedances were kept below 30 kΩ. The EEG signal was pre-amplified at the electrode to improve the signal-to-noise ratio with a gain of 16×, and digitized at 24-bit resolution with a sampling rate of 1024 Hz. Each active electrode was measured online with respect to a common mode sense (CMS) active electrode producing a monopolar (non-differential) channel. All EEG data were analyzed in MATLAB 2012a, using the EEGLAB toolbox (Delorme & Makeig, 2004) and custom code. EEG data were re-referenced off-line to the average of the mastoid channels. Artifactual channels were interpolated with cubic spline interpolation.

In order to preserve the temporal characteristics of the slowly evolving CPP, we adopted a two-stage cleaning procedure. First, to remove drifts, the continuous EEG data were high-pass filtered offline at 0.5 Hz, and segmented from -4.8 s until +1 s surrounding target onset and surrounding response onset. An automatic algorithm detected trials that contained artifacts based on the following criteria: channel joint probability (5.5); channel kurtosis (5.5), and absolute voltage deflections (2 mV). Next, we detected eye-movement and blink artifacts using joint approximation diagonalization of eigen matrices (JADE) independent component analysis (ICA). ICA weights were subsequently stored and projected onto the raw unsegmented data to which no high-pass filter had been applied. The purpose of back projection was to prevent ICA from solely explaining variance due to large drifts in the unfiltered data and thus inaccurately identify eye-blink-related components, and to ensure that trials would not meet artifact rejection criteria due to eye blinks alone.

After removing artifactual ICA components from the unfiltered data, the data were again high-pass filtered (using a two-way least squares FIR filter with a Hanning smoothed kernel), but with a lower frequency cut-off (0.1 Hz) to preserve slow-varying components in the data. The data were segmented, and the automatic artifact detection algorithm was applied, this time with a more stringent absolute voltage deflection criterion (300 µV). All data were then manually checked for residual artifacts and such trials were removed if necessary. Participants for whom <50 trials remained in a single condition were excluded from further analysis to ensure that enough trials remained for single-trial analyses. This applied to 9 participants, making the final sample 21 participants. This exclusion criterion was determined *a priori*, and data of the excluded participants were not analyzed further. Finally, the data were re-referenced to the common average, and converted to current source density to prevent overlap between the CPP and the frontocentral negativity (Kelly & O'Connell, 2013).

CPP identification and parameter estimation. Based on the response-locked scalp topography (Figure 3a) and following prior work (O'Connell et al., 2012; Twomey et al., 2015), all CPP-related analyses were conducted on the average of three centro-parietal EEG channels (P1, P2, and Pz). Significant deviation of the CPP from baseline was examined for each time point from 200 ms pre- to 800 ms post-target onset using permutation testing (10,000 iterations), correcting for multiple comparisons using the false discovery rate (FDR, $q = 0.05$, Figure 3a).

To estimate CPP slope and onset, we fitted a two-part line segment that was connected by a central inflection point (Figure S1) to the data in a window starting at -200 ms pre-stimulus and ending at the time of the response (single-trial analyses) or the peak latency of the CPP (trial-average analyses). The pre-inflection line segment was constrained to have zero slope and amplitude. The two free parameters of this piece-wise function (time of inflection point and slope of post-inflection line) were fit via the Nelder-Mead Simplex optimization routine (via the *fminsearchbnd* MATLAB function), which minimized the sum of squared residuals between the fit and the observed CPP. The latency of the fitted inflection point was taken as the onset latency

of the CPP, and the slope of the line segment following the inflection point was taken as the slope of the CPP. Trials with unrealistic onset latencies (prior to stimulus onset or >600 ms following stimulus onset) and trials with an unrealistic slope (zero or negative) were excluded from analysis. One participant did not show a clear peak in the CPP, so for that participant we used the time of maximum first-order derivative (i.e., the time point where CPP build-up rate started to decline) as a substitute for peak latency for fitting in trial-average analyses. In cases where we used slope in between-participant correlations, we normalized the CPP amplitude across participants to counteract arbitrary differences due to scalp conduction properties, electrode impedances, and other sources of spurious variance prior to computing slope.

Because the fitting window for parameter estimation at the single-trial level varied with RT, and RT in turn varied as a function of task condition, it was conceivable that estimated CPP onset would vary as a function of task condition by chance alone. Therefore, we computed a permuted null distribution by randomly sampling a time point within the fitting window for each trial 10,000 times. We then computed a trial-average value, separately for each condition and iteration of the permutation test, and subsequently averaged across participants. A *p* value for the true participant-average between-condition difference in estimated CPP onset was then computed by counting the number of observations in the permuted null distribution equal to or larger than the true value. Thus, the *p* value reflects the significance of the effect of condition on CPP onset latency, beyond the effect of between-condition differences in the fitting window alone.

Posterior α band power. We used Morlett wavelets to decompose the EEG data into its spectral representation. The wavelets were linearly spaced from 1 to 30 Hz with a cycle range from 3 to 12 (and were defined as in van den Brink, Wynn, & Nieuwenhuis, 2014). Power for each trial was expressed as a percentage change from the average of a 400-ms to 100-ms, frequency-specific, pre-stimulus baseline. We then averaged power in the α band (9-12 Hz) across 14 parieto-occipital channels, selected based on prior work on the relationship between α power and temporal expectations (Rohenkohl & Nobre, 2011).

We first examined if α power was modulated by expectations about stimulus onset by comparing valid to invalid trials with a short CTI, using nonparametric permutation testing (10,000 iterations) and expected larger α power around stimulus onset on invalid trials (i.e., when a target was presented but the participant did not expect it). We then sorted trials by α power in a -25-ms to 75-ms window surrounding target onset (i.e., the earliest window that showed an effect of expectation on α power), computed the average CPP and RT for three bins of trials of equal size, and estimated CPP slope and onset using the fitting procedure described above. We performed the binning procedure for each of the eight conditions of the task design to ensure that a potential relationship between α power and CPP parameters was not driven by between-condition differences in RT that covaried with α power (due to the task design), but instead reflected intrinsic trial-by-trial covariation within a given condition. Finally, for each participant we averaged across the eight conditions and then fitted a straight line to the values of RT, CPP slope and CPP onset across the three bins, and compared the distribution of slopes across participants to zero using permutation testing (10,000 iterations).

Data and code availability. The raw and processed data, as well as code to reproduce the results are publicly available [link inserted upon acceptance].

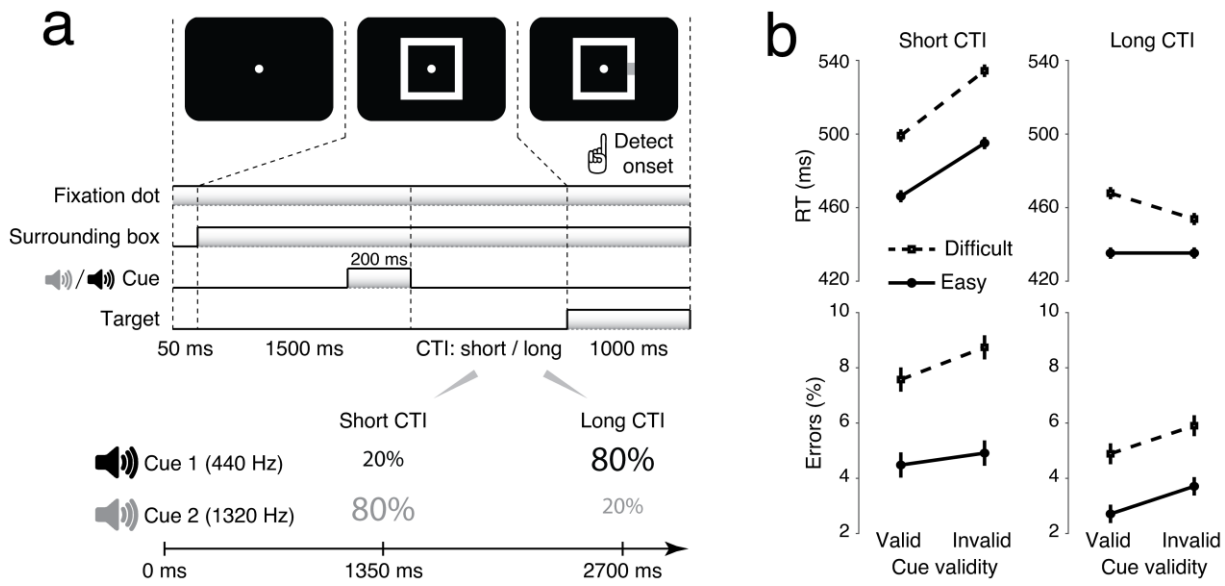

Figure 1. Task and behavioral results. **a)** Task design. **b)** Behavioral results. CTI: cue-target interval RT: response time. Error bars show the within-participant SEM.

RESULTS

Twenty-one individuals each performed 920 trials of a speeded, visual target-detection task in which perceptual difficulty was manipulated by adjusting the luminance of the target stimulus (Figure 1a). Temporal expectations about the timing of the target were manipulated using auditory cues. On each trial, one of two cue tones probabilistically predicted the onset time of the subsequent target. One tone was followed by an early target (1350 ms after the cue) on 80% of the trials and a late target (2700 ms after the cue) on 20% of the trials. For the other tone, these contingencies were reversed. Participants were instructed to use the temporal information signaled by the cue to optimize their RTs.

Temporal expectations influence task performance. The behavioral results were as expected, displaying clear effects of temporal expectation and task difficulty (Figure 1b). Repeated-measures ANOVAs yielded significant main effects on RT and accuracy of validity (RT: $F(1,20) = 9.70$, $p = 0.005$; accuracy: $F(1,20) = 4.48$, $p = 0.047$), CTI (RT: $F(1,20) = 68.33$, $p < 0.001$; accuracy: $F(1,20) = 13.32$, $p = 0.002$), and difficulty (RT: $F(1,20) = 75.40$, $p < 0.001$; accuracy: $F(1,20) = 35.17$, $p < 0.001$). No interaction effects were significant, except the interaction effect of validity and CTI on RT ($F(1,20) = 32.11$, $p < 0.001$). On short CTI trials, participants responded more quickly when they expected the target than when they did not expect it ($t(20) = 6.40$, $p < 0.001$)—the typical temporal cuing effect. On long CTI trials we did not find an effect of cue validity on RT: On invalidly cued long-CTI trials the target hazard rate increases over time, despite a proportion of catch trials, leading participants to reorient their attention toward the long CTI, thus mitigating a temporal cuing effect (Correa et al., 2006). Thus, in line with previous findings (Coull & Nobre, 1998; Nobre et al., 2007), RTs for the short CTI decreased with increasing target probability, indicating that participants used the temporal information conveyed by the cues.

The effect of cue validity at the short CTI (Δ 32 ms, SD 23 ms) and the effect of difficulty (Δ 31 ms, SD 16 ms) were statistically indistinguishable ($t(20) = 0.20$, $p = 0.84$), with a Bayes factor (BF = 0.23) indicating 'substantial' evidence for the null hypothesis of no difference between these effect sizes (Wetzels & Wagenmakers, 2012). This null finding enabled a fair dissociation between the distinct computational parameters that we assumed to underlie these RT effects (see below).

Drift diffusion modelling supports sensory encoding account. We examined the impact of temporal expectations on latent aspects of decision-making by fitting the drift diffusion model (DDM) to participants' behavioral data, using a hierarchical Bayesian model fitting procedure (see *Materials and Methods*; Wiecki et al. 2013). The DDM is a prominent mathematical model of simple decisions like those made in our target-detection task, and can parsimoniously account for RT distributions and choice data across a wide array of tasks (Forstmann et al., 2016). The model assumes that noisy sensory evidence is accumulated over time until one of two opposing bounds is reached, at which point a decision is made in favor of the corresponding decision. In the application of the DDM that we used (Gomez et al., 2007; Zhang et al., 2016), the upper and lower bounds correspond to a 'go decision' (a decision to execute a response, as expected when a target is presented) and an implicit 'no-go decision' (a decision to withhold an overt response, as expected when a target is not presented; Figure 2a). Previous work has found that drift diffusion models with an implicit boundary for no-go decisions provide a better fit of go/no-go task data than single-threshold variants of the model (Gomez et al., 2007). Core DDM parameters include the drift rate, v (which is determined by the quality of the sensory evidence and relates monotonically to the mean rate of evidence accumulation toward the correct decision bound); boundary separation, a (the distance between the two decision bounds, which captures response caution), and non-decision time, T_{er} (the time needed for non-decisional processes capturing sensory encoding and response execution).

To directly contrast the predictions of the sensory encoding account of temporal expectations with an account wherein expectations affect evidence quality (and thus accumulation rate), we examined a model fit to data from short CTI trials in which non-decision time (T_{er}) and drift rate (v) were free to vary as a function of cue validity. Drift rate was also free to vary as a function of difficulty, in line with common findings that differences in stimulus strength in perceptual tasks are well captured by this parameter (Ratcliff, 2002). The model accurately reproduced empirically observed RTs, with correlation coefficients between condition-specific mean RTs in data and model > 0.84, and empirical data fell within the 95th percentile credibility interval of the model (Figure 2b). Model fits showed a significant difference in T_{er} between valid and invalid trials (p = 0.002, Figure 2c), indicating a temporal expectation effect on non-decisional processes. In contrast, v did not differ between valid and invalid trials (p = 0.30; Figure 2d), which is inconsistent with the evidence quality account of temporal expectations. Instead, as expected, v differed between easy and difficult trials (p = 0.004; collapsed across validity conditions).

Several features of our results showed that the effect of cue validity on RT was primarily driven by a change in T_{er}. First, the effect of cue validity on T_{er} (Δ 29 ms, SD 17 ms) and the effect of cue validity on RT (Δ 32 ms, SD 23 ms) were statistically indistinguishable (BF = 0.30). Second, the participant-specific effect of cue validity on RT was positively correlated with the effect of cue validity on T_{er} (r = 0.64, p = 0.002; Figure 2e). Moreover, the slope of the least squares regression line that captured this relationship (0.87; 95% confidence interval determined via bootstrapping: 0.42 – 1.17) did not differ from the slope of the identity line (1.00, reflecting an idealized case where the cuing effect on RT is fully captured by T_{er}). While a cross-subject correlation between the effects of difficulty on RT and on v was also significant (r = -0.63, p = 0.002), by contrast, there was no significant correlation between the effects of cue validity on v and RT (r = 0.32, p = 0.17). Together, these findings show that T_{er}, not v, was the primary factor that drove the cue-validity effect on RT.

To further assess the effect of temporal expectations on the different model parameters, we compared a range of models (including the model described above) that differed with regard to which parameter or combination of parameters was allowed to vary as a function of cue validity. In all models, v was free to vary as a function of difficulty. To compare the adequacy of the eight models in explaining the observed data we used the DIC metric, a statistical criterion for model selection that takes into account model complexity. As can be seen in Table 1, the model in which only T_{er} was free to vary between valid and invalid trials provided the best fit of the data—a significantly better fit than the model ranked second ($T_{er} + a + v$, ΔDIC = 10) and the v-only model (ΔDIC = 179). Notably, the four best fitting models were all of the models in which T_{er} was allowed to vary between valid and invalid trials. Thus, our DDM analyses strongly supported an account whereby temporal

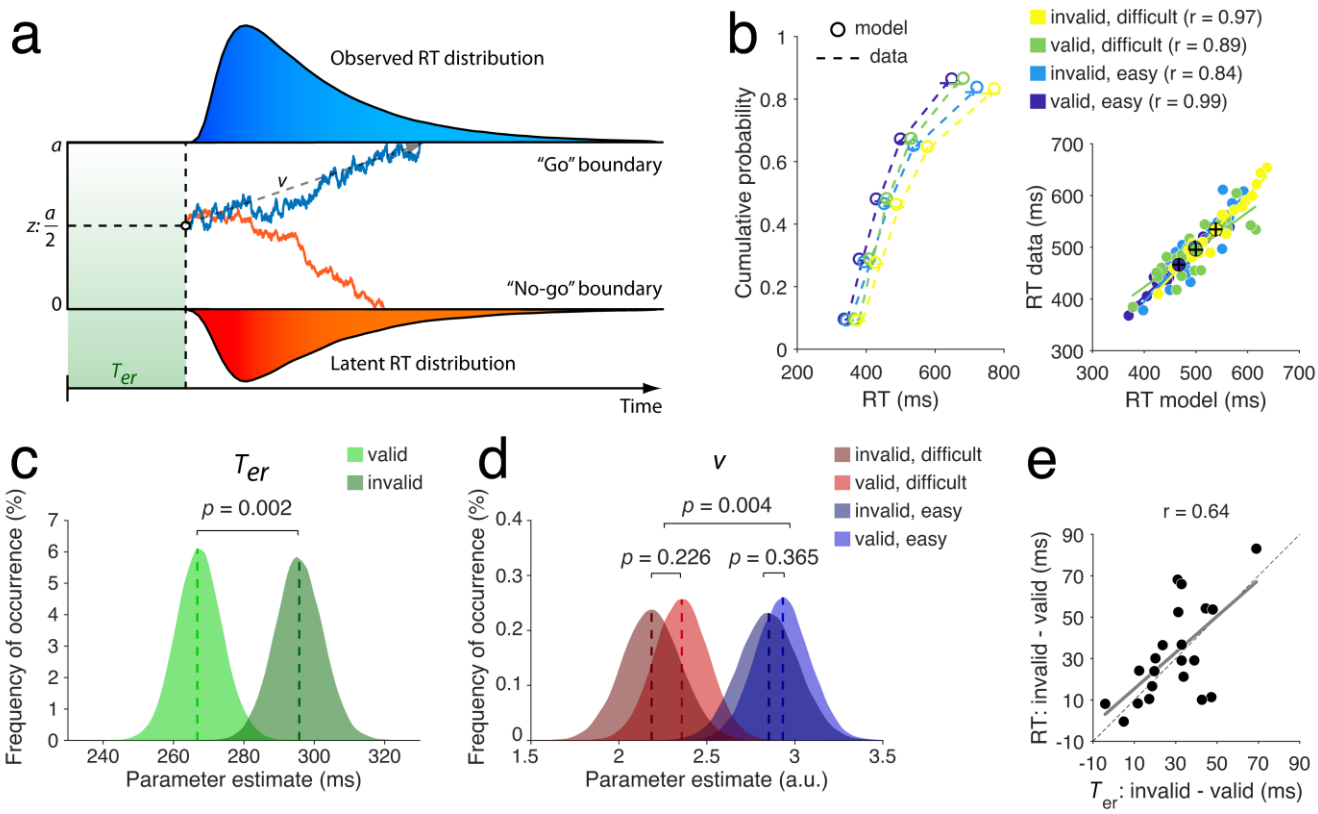

Figure 2. Hierarchical drift diffusion modeling results. **a)** Schematic and example traces of the go/no-go drift diffusion model. Following a period of non-decision time (T_{er}), noisy evidence accumulates over time at mean drift rate (v) until a threshold (0 or a) is reached. In our implementation, starting point (z) was unbiased. **b)** Empirical (data) and simulated (model) defective cumulative quantile probability (left) and mean response times (right). In the right panel, small dots show individual participants. Large dots show the group means. Error bars show the within-participant SEM. **c)** Non-decision time (T_{er}) differed between valid and invalid trials. **d)** Drift rate (v) did not differ between valid and invalid trials, but did differ between easy and difficult trials. Vertical dotted lines in c) and d) show the average of the participant-specific maximum *a-posteriori* parameter estimates. Distributions show the group posterior. Statistical significance is reflected in the overlap between distributions. **e)** Across-participant correlation between the effects of cue validity on RT and T_{er}. The dotted line shows the identity line. The solid gray line shows a least-squares regression line.

Table 1. Models ranked in terms of deviance information criterion

v ~ difficulty	v ~ validity	a ~ validity	T_{er} ~ validity	DIC
X			X	-7622
X	X	X	X	-7612
X	X		X	-7605*
X		X	X	-7595
X		X		-7523
X	X			-7443
X				-7405

Abbreviations: v: drift rate, a: boundary separation, T_{er}: non-decision time, DIC: deviance information criterion (more negative = better fit), ~: free to vary as a function of, *: primary model used to contrast the two competing accounts.

expectations selectively act to hasten non-decisional processes, but do not affect the process of evidence accumulation itself.

Target detection is associated with an electrophysiological signature of decision making. Previous work has identified an electrophysiological signature of evidence accumulation during decision making tasks: a supramodal, motor-independent centroparietal positivity (CPP) in the event-related potential that exhibits the typical dynamics of a build-to-threshold decision signal (Kelly & O'Connell, 2013; O'Connell et al., 2012; Twomey et al., 2015). The CPP thus provided us with a neural measure by which to examine the effect of temporal expectation on decision formation (Loughnane et al., 2016).

In line with previous work, the CPP in our data showed a significant ($p < 0.05$, FDR-corrected), gradual build-up following target onset, peaked around the time of the response, and was maximal over centroparietal electrodes (Figure 3a). Moreover, the CPP was uncontaminated by visual-evoked potentials, as our task was designed to minimize sensory transients. The CPP also exhibited the typical relationship with RT that might be expected from a build-to-threshold decision variable signal. Specifically, we split each participant's RT distribution into equal-sized fast, medium and slow bins (within task conditions) and plotted the average waveforms aligned to target presentation and response execution for each bin (Figure 3b). Consistent with previous observations (Kelly & O'Connell, 2013; O'Connell et al., 2012) the onset and peak latencies of the stimulus-locked CPP directly scaled with RT, while its slope (i.e., build-up rate) was inversely proportional to RT (see Figure S2 for fits of individual participants, and cross-participant correlations with behavior and model parameters). Furthermore, the response-locked CPP reached a stereotyped amplitude at the time of response execution, consistent with the notion of fixed decision bounds.

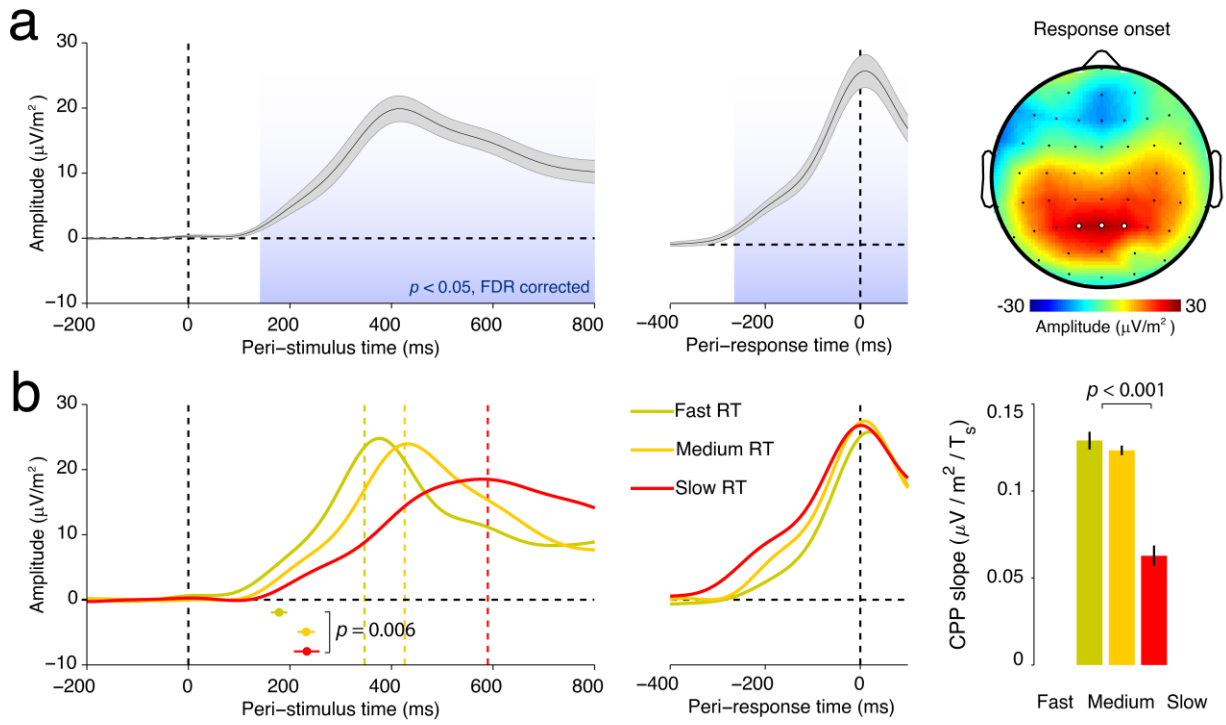

Figure 3. Condition-average CPP. **a)** Stimulus- and response-locked CPP waveforms and scalp topography. Shaded regions show the within-participant SEM. The highlighted electrodes, P1, P2 and Pz, were used for all analyses. **b)** CPP characteristics scale with response time (RT). Single trials were sorted as a function of RT and divided into equal-sized fast, medium and slow bins, separately for each participant and task condition, then averaged. Colored vertical dotted lines show the average RT per bin. Dots below the traces show the CPP onset latency. Error bars show the within-participant SEM.

Temporal expectation and task difficulty have dissociable effects on CPP onset latency and slope. The sensory encoding account predicts that temporal expectation reduces the onset latency of the CPP, which reflects the time needed for sensory encoding. In contrast, an effect of temporal expectation on evidence quality predicts a steeper slope (i.e., build-up rate) of the CPP (Kelly & O'Connell, 2013). Trial-average analyses (Figure 4a, b) provided preliminary support for the sensory encoding account. Cue validity showed a trend-level effect on onset latency in the expected direction (p = 0.097), but no effect on slope (p = 0.555). In contrast, difficulty affected the CPP slope (p = 0.010), reflecting the expected shallower CPP slope on difficult trials, but not the onset latency (p = 0.775). This also indicated that the absence of an effect of cue validity on CPP slope was not due to a lack of sensitivity in accurately measuring CPP slope, because task difficulty and cue validity had a comparable effect on RT. Furthermore, the latency between the peak of the response-aligned CPP and the motor response (a proxy for the time between decision and response execution) did not differ between valid and invalid trials (p = 0.31, BF = 0.38). This suggested that the effect of cue validity on T_{er} (see previous section) was unlikely to be due to between-condition differences in post-decisional processing, and instead likely reflected sensory encoding time.

The trial-average analyses may have underestimated the true effect of validity on CPP onset latency if invalid short-CTI trials (in which the early target was not expected) were associated with larger trial-by-trial variability in onset latency. In that case, the wider left tail of the distribution for invalid trials would have led to an earlier onset of the trial-averaged CPP, diminishing the difference in CPP onset latency between valid and invalid trials. To examine this possibility, we computed single-trial measures of CPP onset latency and slope (see *Materials and Methods*). These data confirmed that invalidly cued short-CTI trials were associated with increased variability in onset latency compared to validly cued short-CTI trials (p = 0.003, Figure 4c), suggesting that our key predictions might be addressed more reliably using single-trial analyses.

Thus, to avoid spurious effects of trial-to-trial variability on the shape of the trial-average CPP waveform, we examined the effects of temporal expectation and task difficulty on single-trial measures of CPP onset latency and CPP slope (Figure 4c). These analyses revealed that the CPP onset latency was significantly shorter on validly cued trials than on invalidly cued trials (p = 0.008), while the CPP slope did not differ (p = 0.480). As expected, and in line with the trial-average analyses, CPP slope was shallower for difficult trials than for easy trials (p = 0.021).

Our finding of a cue-validity effect on CPP onset latency is consistent with the notion that temporal expectation hastens sensory encoding. However, an alternative possibility is that on validly cued (versus invalidly cued) short-CTI trials, when the target was expected to appear after the short CTI, participants engaged in premature sampling (of noise) on a proportion of the trials (Jepma, Wagenmakers, & Nieuwenhuis, 2012; Laming, 1979; Devine et al., 2019). That is, participants may anticipate the arrival of a target stimulus and speed up responses by starting to sample information from the display at the moment when they think the stimulus will be presented. On a proportion of the trials they may start sampling too early, and if these premature sampling trials are included in the analysis, the average single-trial CPP onset latency may give the impression of speeded sensory encoding.

Premature sampling should lead to faster but less accurate responses, because participants will start with sampling noise. Accordingly, we discouraged premature sampling by instructing participants to avoid response errors and aborting trials on which responses were made before target onset. Anticipations were not more common on short-CTI trials when a target was expected, compared to when a target was not expected ($t(20)$ = 1.39, p = 0.18, BF = 0.52) suggesting that any premature sampling that participants may have engaged in was not modulated by temporal expectation. To further rule out a role for premature sampling, we carried out a control analysis, focusing on the ERP waveform associated with invalidly cued long-CTI trials. On these trials participants expected the target to occur after the short CTI. Premature sampling (relative to the expected target onset latency) should result in a positive "pre-target" CPP deflection that cannot possibly reflect evoked activity, given that the target is not presented at the expected time. However, our control analysis did not yield any support for this prediction (Figure S3).

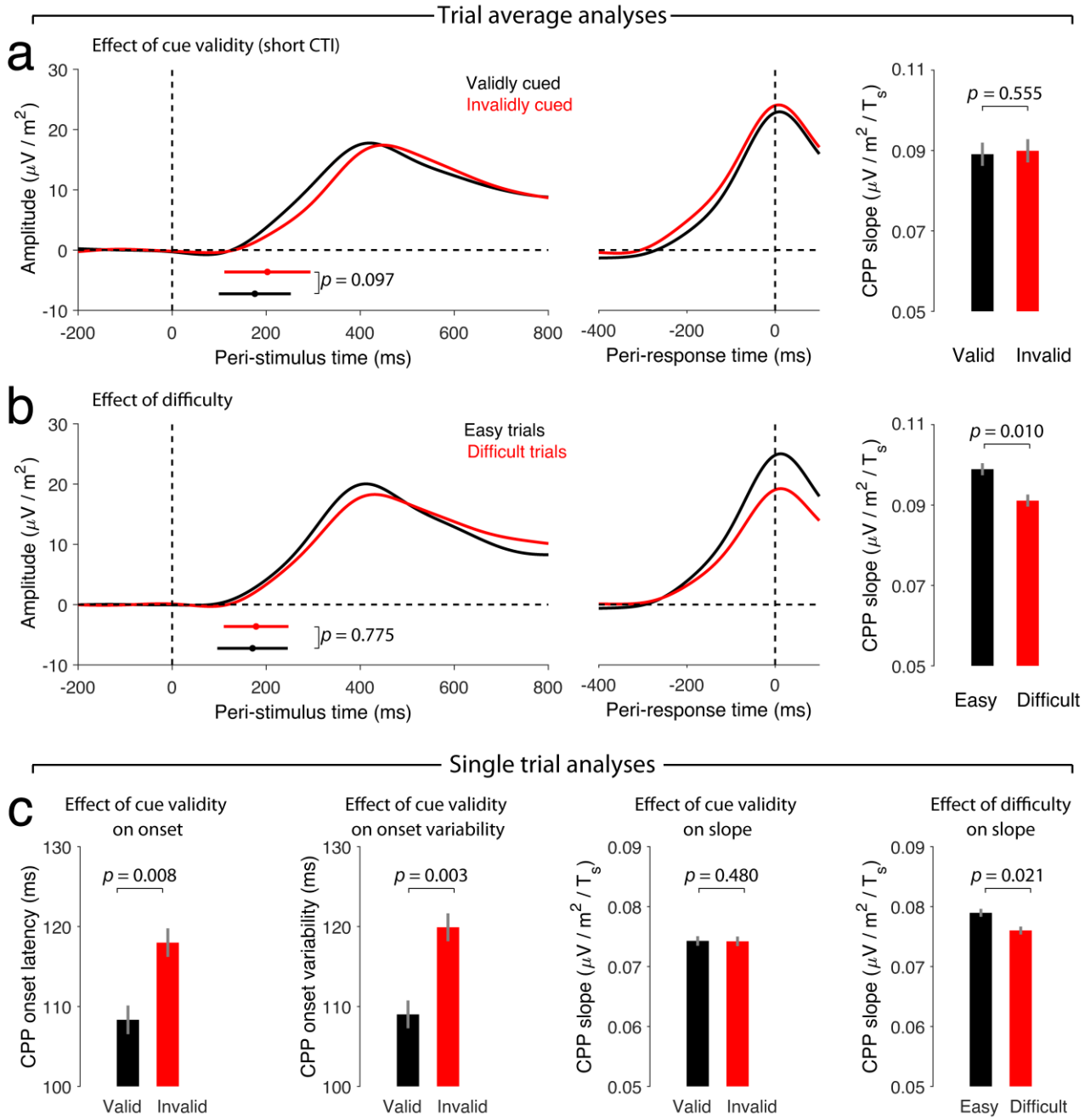

Figure 4. Effects of cue validity and difficulty on the CPP. **a)** Effect of cue validity, and **b)** difficulty on the trial-averaged CPP. Dots and lines below the ERP waveforms show the average estimated CPP onset latency and SD across participants. **c)** Comparison between CPP measures extracted at the single-trial level. Error bars in bar graphs reflect the within-participant SEM.

CPP onset latency covaries with behaviorally relevant fluctuations in peri-stimulus α power. In search of a mechanism underlying the effect of temporal expectations on sensory encoding, we examined a potential endogenous determinant of CPP onset latency that might account for trial-to-trial variability in CPP onset latency and corresponding fluctuations in task performance. In particular, we used EEG time-frequency analysis to examine the power of ongoing neural oscillations in the α band (9-12 Hz) over posterior cortical areas, reflecting rhythmic fluctuations in cortical excitability (Jensen & Mazaheri, 2010; Pfurtscheller, 2001). A large number of studies have found that the amplitude of α-band oscillations around the onset time of a target stimulus predicts subsequent task performance (Ergenoglu et al., 2004; Mathewson, Gratton, Fabiani, Beck, & Ro, 2009; Thut et al., 2006; van Dijk, Schoffelen, Oostenveld, & Jensen, 2008), in line with the well-accepted notion that the neural and behavioral responses to a stimulus depend on the cortical state at the time of stimulus presentation. Importantly, the power and phase of α-band oscillations around the time of a stimulus can be modulated by top-down attention to optimize the processing of that stimulus (Samaha, Bauer, Cimaroli, & Postle, 2015; van Diepen, Cohen, Denys, & Mazaheri, 2015).

The top-down modulation of the power of oscillatory α-band activity has been proposed to play a pivotal role in performance on temporal expectation tasks. Previous EEG research has found that α power is reduced just prior to, or at, the expected onset time of a target event (Breska & Deouell, 2017; Praamstra, Kourtis, Kwok, & Oostenveld, 2006; Rohenkohl & Nobre, 2011), yielding enhanced cortical excitability over the time interval in which the target event is expected. This signature of temporally focused attention, often referred to as α desynchronization, was also present in our data. Power in the α band was maximal over posterior scalp regions (Figure 5a) and specifically posterior α was modulated by expectations about stimulus onset (Figure 5b), leading us to ask whether fluctuations in this signal were associated with fluctuations in CPP onset latency, our neural marker of sensory encoding time. To address this question we binned trials based on single-trial, peri-stimulus posterior α power within each cell of the task design, and then averaged across cells to make sure that any difference between bins in α power was unrelated to task manipulations, including the cue validity manipulation, but instead reflected endogenous trial-by-trial variability.

A statistical comparison between bins indicated that the differences in peri-stimulus posterior α power were behaviorally relevant, as decreases in α power were associated with faster RTs (Figure 5c; $p < 0.001$). Importantly, decreased α power was also associated with a reduced CPP onset latency, indicating faster sensory encoding ($p = 0.039$), but not with differences in CPP slope ($p = 0.855$) (Figure 5c). Identical results in terms of direction and significance were found using an alternate frequency band (9-14 Hz). As expected, long CTI trials, which showed no significant effect of cue validity on RT, also showed no significant effect of cue validity on α power (Figure S4). Combined, our results indicate that top-down modulation of α-band activity putatively modulates cortical excitability in a way that expedites the sensory encoding of expected stimuli.

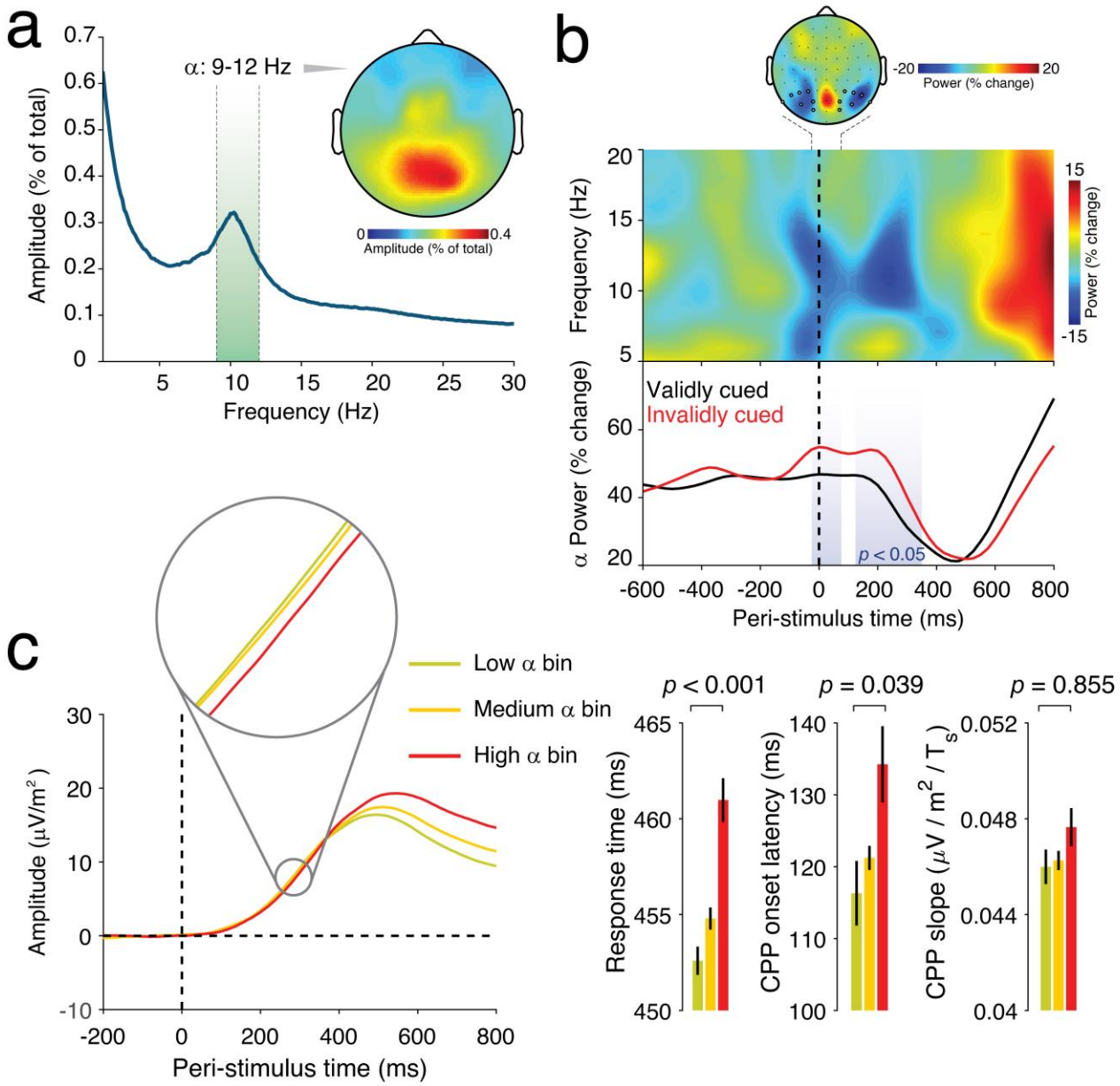

Figure 5. Relationship between posterior α (9-12 Hz) power, temporal expectations and CPP parameters. **a)** Power spectrum and topography of α power. **b)** Comparison of power across time and frequency for valid versus invalid trials. Blue colors indicate lower power for valid trials. The topographical plot shows effect of cue validity on power in the α (9-12 Hz) band; highlighted channels are those averaged over to create remaining panels, chosen independently, based on Rohenkohl and Nobre (2011). **c)** Trial-averaged CPP binned by peri-stimulus α power (*left*), and effect of α bins on RT, CPP onset latency and CPP slope (*right*). Error bars show the within-subject SEM.

DISCUSSION

Temporal contingencies in sensory input, such as music, speech and other temporal sequences, provide a critical source for temporal predictions formed in the brain, considerably improving the speed and accuracy of responding to unfolding events. Here, we used mathematical modelling of behavior and neural signal measurements to identify how temporal expectations enhance perception.

All model-based analyses suggested that the cue-validity effect, our behavioral measure of temporal expectations, was specifically driven by changes in non-decisional processes (T_{er}), and not by possible effects on the decision process (including an effect on evidence quality and, accordingly, the mean rate of accumulation, v). Specifically, model fits as well as model-selection procedures supported the T_{er} account. Furthermore, the cue-validity effects on T_{er} and RT were highly correlated and almost identical in size. No such support was obtained for an account whereby temporal expectations enhance the quality of the sensory evidence (Rohenkohl et al., 2012a). Although non-decision time includes the time needed for both sensory encoding and response execution, previous studies have found that temporal expectations have negligible effects on response execution time, as indicated by the interval between the onset of the lateralized readiness potential and the overt response (Hackley, Schankin, Wohlschlaeger, & Wascher, 2007; Müller-Gethmann, Ulrich, & Rinkenauer, 2003; but see Tandonnet, Burle, Vidal, & Hasbroucq, 2006). Likewise, we found that the time difference between the peak latency of the CPP and the motor response, a proxy for the duration of response execution, did not differ between valid and invalid trials. Together, these results indicate that our temporal expectation effect on T_{er} primarily reflects sensory encoding time, not post-decisional processing time.

Our study is the first to complement mathematical modelling with detailed EEG analyses regarding the effects of temporal expectation on decisional and nondecisional process. Such neural evidence is critical, given reported discrepancies between results from sequential-sampling models and neural signatures of decision formation (McGovern et al., 2018; Spieser et al., 2018). These additional analyses of the CPP allowed us to examine the effect of temporal expectation on the onset and rate of decision formation in the brain (Loughnane et al., 2016), and yielded further support for the sensory encoding account. Single-trial analyses, necessary to avoid a measurement artifact in the trial-average CPP, revealed a shortened CPP onset latency on validly cued trials, consistent with the notion that temporal expectation hastens sensory encoding. In contrast, valid and invalid trials did not differ in CPP slope, suggesting that temporal expectation did not affect the quality of the sensory evidence or other processes influencing the rate of decision formation. Control analyses excluded premature sampling of the stimulus array prior to target onset (Jepma et al., 2012; Laming, 1979; Devine et al., 2019) as an alternative explanation of these results.

EEG α-band power is thought to reflect local cortical excitability (Jensen & Mazaheri, 2010; Pfurtscheller, 2001) and has previously been shown to track temporal expectations, enhancing perception of events occurring at expected moments (Ergenoglu et al., 2004; Mathewson et al., 2009; Thut et al., 2006; van Dijk et al., 2008). In our study, peri-stimulus posterior α power was also behaviorally relevant, showing a strong positive relationship with RTs. The novel insight provided by our data was that peri-stimulus α power also covaried with CPP onset latency (and not with CPP slope), suggesting that peri-stimulus posterior α power is a key determinant of sensory encoding time, presumably contributing to the perceptual facilitation associated with temporal expectation. This facilitation may be brought about by top-down signals that modulate visual cortex activity in order to expedite target processing, and result in an earlier start of the decision process (and therefore a shorter CPP onset latency). Notably, α is the dominant frequency band for feedback signaling from higher-order cortical regions to lower-level visual cortex (Michalareas et al., 2016; van Kerkoerle et al., 2014). Thus, it is possible that α power is a signature of a top-down modulatory process: co-variation between posterior α power and CPP onset latency may reflect fluctuations in top-down signaling in accordance with expectations about target onset.

There are prominent discrepancies between the current results and previously published model-based analyses of behavioral temporal expectation effects (Cravo et al. 2013; Rohenkohl et al., 2012a; Vangkilde et

al., 2012). Vangkilde and colleagues (2012) found that temporal expectations enhanced (unspeeded) visual letter discrimination and analyzed these behavioral data using the *theory of visual attention* (TVA). These analyses suggested that the improvement in perceptual discrimination was caused by an increased rate of evidence accumulation (TVA parameter: perceptual processing speed), and not by faster sensory encoding (TVA parameter: temporal threshold for conscious perception). Likewise, Nobre and colleagues found that temporal expectations enhanced visual contrast sensitivity, and reported fits of a sequential-sampling model suggesting that this enhancement in perceptual discrimination was caused by an increased quality of the sensory evidence (Cravo et al. 2013; Rohenkohl et al., 2012a).

Nobre and colleagues (Cravo et al. 2013; Rohenkohl et al., 2012a) modeled their behavioral data using a diffusion model that was developed to simultaneously fit psychometric (accuracy) and chronometric (RT) functions (Palmer, Huk, & Shadlen, 2005). However, we argue that this diffusion model was not entirely appropriate with regard to the task performed by the participants. Specifically, in both studies participants were asked to discriminate the orientation of visual gratings (Gabor patches) at seven contrast levels, resulting in accuracy levels spanning from near chance to near perfect. Each trial consisted of a stream of noise patches and infrequent visual gratings (targets) presented either with a fixed, rhythmic (high temporal expectation) or jittered, arrhythmic (low temporal expectation) stimulus onset asynchrony. Critically, each target was presented for only 50 ms and then followed by a noise patch after 350 ms. This means that the task potentially violated an assumption underlying the diffusion model of Palmer and colleagues, namely that the evidence on the screen does not change during the decision process. The consequences of the violation of this stationarity assumption are unclear. The brief target duration and the short time until the next noise patch meant that on that task, there was very limited time for participants to secure a robust visual short-term memory trace of the decision-relevant stimulus feature, which in turn provides input to the decision process once the stimulus is no longer visible (cf. Ratcliff, Smith, Brown, & McKoon, 2016; Rohenkohl et al., 2012b; Smith & Ratcliff, 2009). In such conditions, expedited sensory encoding could well be beneficial for discrimination accuracy in that it would allow more time for the creation of a high-quality memory trace before the perturbance of the subsequent noise patch (cf. Nieuwenhuis, Jepma, & Wagenmakers, 2012; Rolke & Hofmann, 2007). Importantly, such a change in accuracy is often diagnostic of a change in drift rate, while generally inconsistent with a change in nondecision time. Thus, a potentially violated assumption may have led the model to misattribute an effect on sensory encoding time to a change in drift rate. Taken together, these arguments invite caution when interpreting previous modelling results (Cravo et al. 2013; Rohenkohl et al., 2012a) in terms that are explicit about the locus of the effect of temporal expectation on performance.

The discrepancy between our results and those of Vangkilde and colleagues (2012) also deserves further theoretical consideration. To our knowledge, the formal relationship between diffusion models and the TVA, including the mapping between their model parameters, has not been studied yet. Given the model assumption and mimicry issues discussed here, it is critical that we obtained solid neural evidence for the sensory encoding account.

Another plausible explanation for the discrepancy between the current results and previous work concerns differences between studies in the structure of temporal information provided to participants. Nobre and van Ede (2017) distinguish four types of informative temporal structures that are commonly found in the environment and manipulated in experimental tasks: (i) temporal associations—that is, predictive temporal relations between successive stimuli, such as the auditory cue and the visual target in our study; (ii) hazard rates; (iii) rhythms; and (iv) sequences—recurring temporal structures that are more complex than simple rhythms. Although there is some evidence that temporal expectations based on these structures rely on similar brain mechanisms (Breska & Deouell, 2017; Correa & Nobre, 2008), the differences and similarities between the types of temporal structures and associated brain mechanisms are only beginning to be investigated (Nobre & van Ede, 2017; Shalev, Nobre, & van Ede, 2019). Interestingly, the manipulations of temporal expectation of Vangkilde and colleagues (2012) and Nobre and colleagues (Cravo et al. 2013; Rohenkohl et al., 2012a) were based on hazard rates and rhythms, respectively. In contrast, behavioral studies that used

temporal associations (i.e., temporal cuing or a foreperiod manipulation) have reported evidence that temporal expectations specifically affect the duration of sensory encoding and not the decision process (Bausenhart et al., 2010; Seibold et al., 2011). Future research should examine the possibility that different types of temporal structures call upon dissociable temporal expectation mechanisms.

Our findings contribute to a growing literature documenting the usefulness of the CPP as a neural marker of perceptual decision formation (O'Connell et al., 2018), but there are also important outstanding questions regarding the methodological limitations and functional significance of the CPP (Urai & Pfeffer, 2014). Furthermore, recent work has put forward the peak latency of the N200 component as an alternative EEG marker of the onset of the evidence accumulation process (Nunez, Gosai, Vandekerckhove, & Srinivasan, 2019). In addition, although our study focused on perception, there is marked evidence that temporal expectation can also affect aspects of motor processing (e.g., Fecteau & Munoz, 2007; Hackley & Valle-Inclán, 2003; Nobre et al., 2007), albeit perhaps not the *duration* of these processes. Lastly, future research may shed more light on the precise mechanistic origin of trial-by-trial co-fluctuations in posterior α power around the time of stimulus presentation and the onset of decision formation.

SUPPLEMENTARY FIGURES

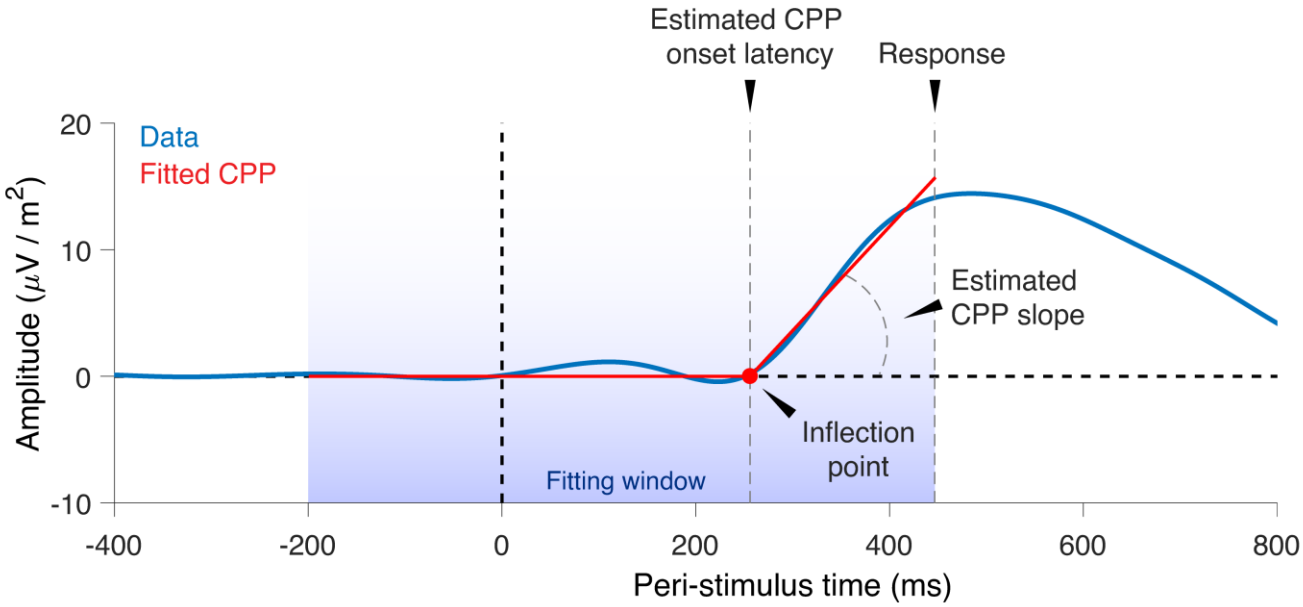

Figure S1. Method for estimating CPP slope and onset. Two straight lines that share an inflection point were fitted to the data with the constraint that the pre-onset part must have a slope and amplitude of zero, and the post-onset part must have a positive slope. The window for fitting was from 200 ms before stimulus onset until the time of response (for single-trial analyses) or until the peak latency of the CPP (for trial-average analyses).

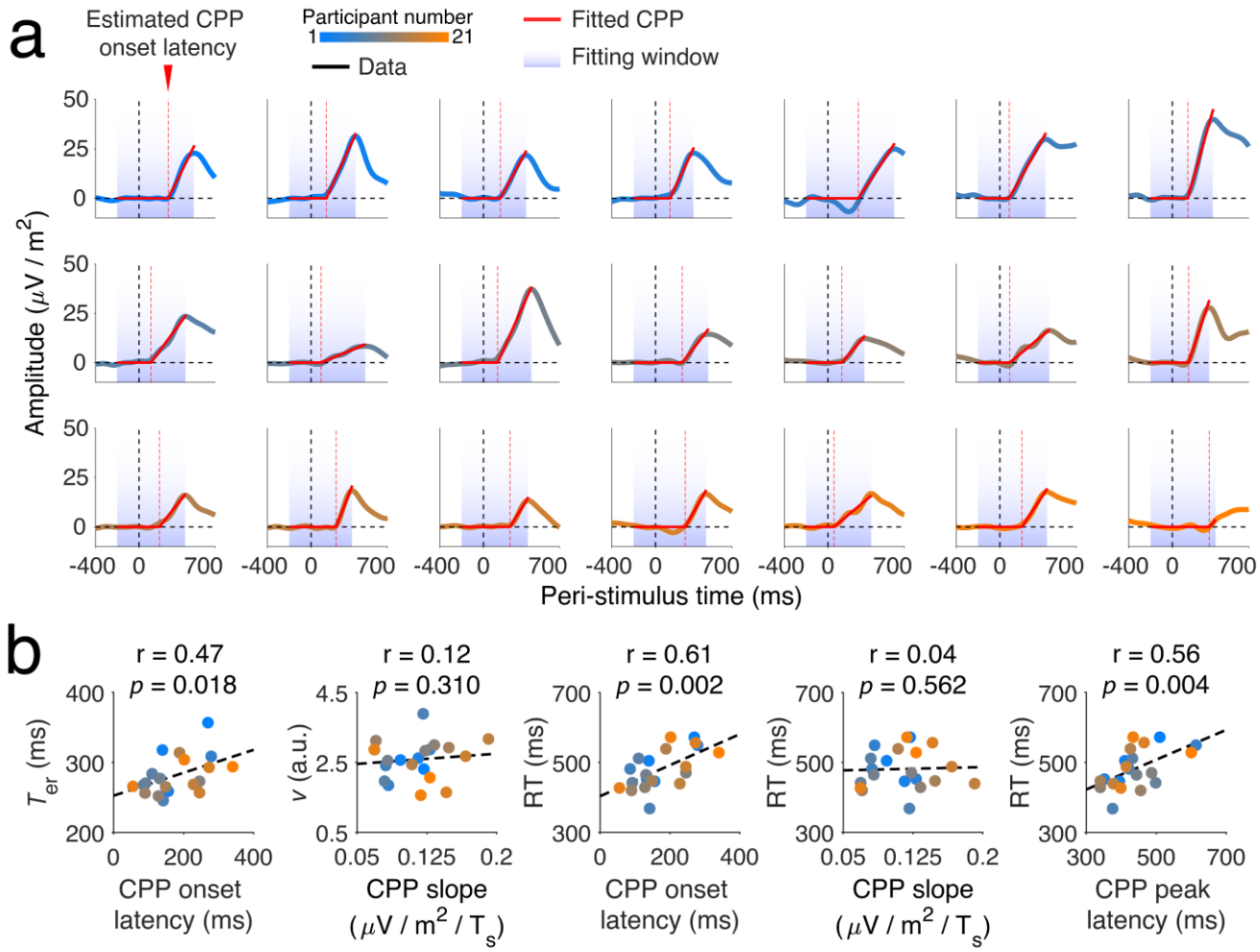

Figure S2. CPP fits per participant, and relationship with other measures. **a)** Condition-averaged CPP for each participant. Solid red lines show the fitted CPP traces. Red dashed lines show the estimated CPP onset latency. **b)** Cross-participant correlations between model parameters, response time (RT), and three CPP measures: CPP onset latency, CPP slope, and CPP peak latency. Prior to estimating slope, the individual CPP curves were scaled to fixed height to correct for arbitrary amplitude differences between participants.

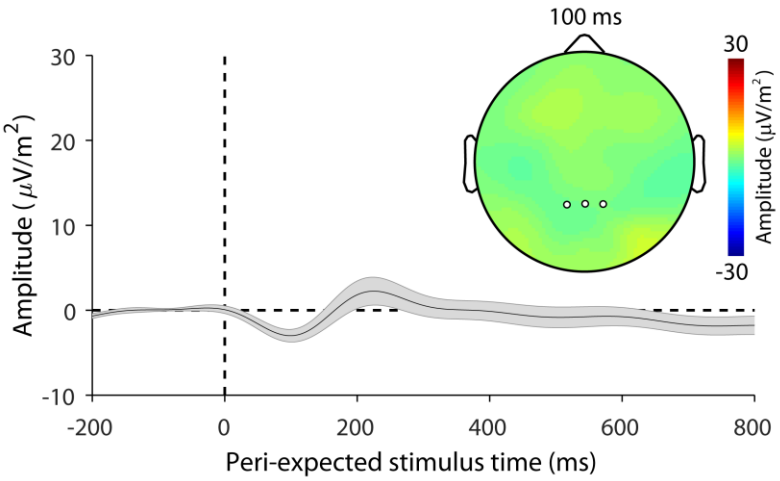

Figure S3. Control analysis to rule out premature sampling. The figure shows the ERP for invalid long-CTI trials, at the time points surrounding the short CTI (i.e., when a target was expected, but not presented). If participants were starting to accumulate evidence prior to stimulus onset, we would expect to see a positive deflection around stimulus onset, but no time points were significantly different from zero (all FDR $p > 0.05$). Color and axis limits are as in Figure 3a in the main text.

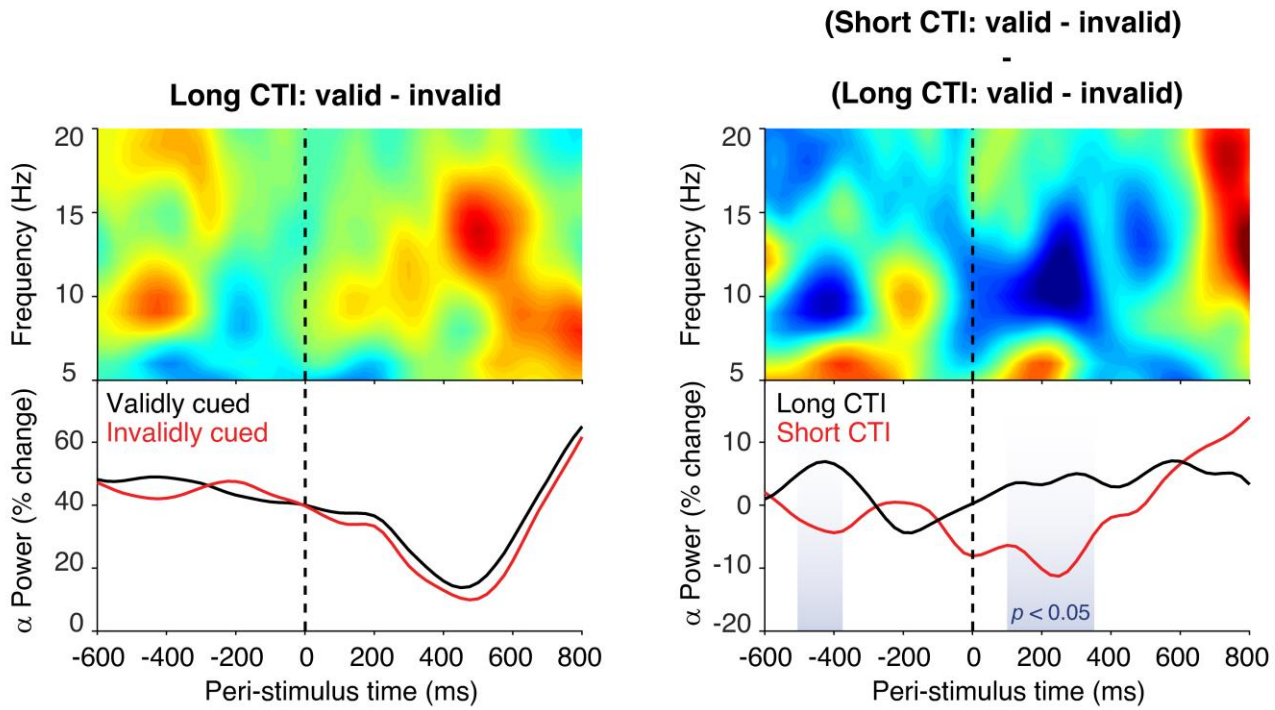

Figure S4. Comparison of posterior α (9-12 Hz) power across time and frequency for valid versus invalid trials with a long CTI (left) and interaction with short CTI (right).

REFERENCES

Bausenhart, K. M., Rolke, B., Seibold, V. C., & Ulrich, R. (2010). Temporal preparation influences the dynamics of information processing: Evidence for early onset of information accumulatnion. *Vision Research, 50,* 1025-1034.

Breska, A. & Deouell, L.Y. (2017). Neural mechanisms of rhythm-based temporal prediction: Delta phase-locking reflects temporal predictability but not rhythmic entrainment. *PLoS Biology, 15,* e2001665.

Busch, N.A., Dubois, J. & VanRullen, R. (2009). The phase of ongoing EEG oscillations predicts visual perception. *Journal of Neuroscience, 29,* 7869-7876.

Correa, A., Lupiáñez, J., Madrid, E., & Tudela, P. (2006). Temporal attention enhances early visual processing: a review and new evidence from event-related potentials. *Brain Research, 1076,* 116-128.

Correa, A., Lupiáñez, J., Milliken, B., & Tudela, P. (2004). Endogenous temporal orienting of attention in detection and discrimination tasks. *Perception & Psychophysics, 66,* 264-278.

Correa, A., Lupiáñez, J., & Tudela, P. (2005). Attentional preparation based on temporal expectancy modulates processing at the perceptual level. *Psychonomic Bulletin & Review, 12,* 328-334.

Correa, A., Lupiáñez, J., & Tudela, P. (2006). The attentional mechanism of temporal orienting: determinants and attributes. *Experimental Brain Research, 169,* 58-68.

Correa, A., & Nobre, A.C. (2008). Neural modulation by regularity and passage of time. *Journal of Neurophysiology, 100,* 1649-1655.

Coull, J.T., & Nobre, A.C. (1998). Where and when to pay attention: the neural systems for directing attention to spatial locations and to time intervals as revealed by both PET and fMRI. *Journal of Neuroscience, 18,* 7426-7435.

Cravo, A.M., Rohenkohl, G., Wyart, V., & Nobre, A.C. (2013). Temporal expectation enhances contrast sensitivity by phase entrainment of low-frequency oscillations in visual cortex. *Journal of Neuroscience, 33,* 4002-4010.

Devine, C.A., Gaffney, C., Loughnane, G.M., Kelly, S.P., O'Connell, R.G. (2019). The role of premature evidence accumulation in making difficult perceptual decisions under temporal uncertainty. *eLife*, *8*, e48526

Ergenoglu, T., Demiralp, T., Bayraktaroglu, Z., Ergen, M., Beydagi, H., & Uresin, Y. (2004). Alpha rhythm of the EEG modulates visual detection performance in humans. *Cognitive Brain Research, 20,* 376-383.

Fecteau, J.H. & Munoz, D.P. (2007). Warning signals influence motor processing. *Journal of Neurophysiology, 97,* 1600-1609.

Forstmann, B.U., Ratcliff, R., & Wagenmakers, E.J. (2016). Sequential sampling models in cognitive neuroscience: Advantages, applications, and extensions. *Annual Reviews in Psychology, 67,* 641-666.

Gold, J.I., & Shadlen, M.N. (2007). The neural basis of decision making. *Annual Review of Neuroscience, 30,* 535-574.

Gomez, P., Ratcliff, R., & Perea, M. (2007). A model of the go/no-go task. *Journal of Experimental Psychology: General, 136,* 389–413.

Hackley, S.A., & Valle-Inclán, F. (2003). Which stages of processing are speeded by a warning signal? *Biological Psychology, 64,* 27-45.

Hackley, S. A., Schankin, A., Wohlschlaeger, A., & Wascher, E. (2007). Localization of temporal preparation effects via trisected reaction time. *Psychophysiology, 44,* 334–338.

Henry, M.J., Herrmann, B., & Obleser, J. (2014). Entrained neural oscillations in multiple frequency bands comodulate behavior. Proceedings of the National Academy of Sciences, 111, 14935-14940.

Huk, A.C., & Shadlen, M.N. (2005). Neural activity in macaque parietal cortex reflects temporal integration of visual motion signals during perceptual decision making. *Journal of Neuroscience, 25,* 10420-10436.

JASP Team (2019). JASP (Version 0.9.2)[Computer software]

Jepma, M., Wagenmakers, E.-J., & Nieuwenhuis, S. (2012). Temporal expectation and information processing: A model-based analysis. *Cognition, 122,* 426-441.

Kelly, S.P., & O'Connell, R.G. (2013). Internal and external influences on the rate of sensory evidence accumulation in the human brain. *Journal of Neuroscience, 33,* 19434-19441.

Laming, D. (1979). Choice reaction performance following an error. *Acta Psychologica, 43,* 199–224.

Loughnane, G.M., Newman, D.P., Bellgrove, M.A., Lalor, E.C., Kelly, S.P., & O'Connell, R.G. (2016). Target selection signals influence perceptual decisions by modulating the onset and rate of evidence accumulation. *Current Biology, 26,* 496-502.

Mathewson, K.E., Gratton, G., Fabiani, M., Beck, D.M., & Ro, T. (2009). To see or not to see: prestimulus alpha phase predicts visual awareness. *Journal of Neuroscience, 29,* 2725-2732.

McGovern, D.P., Hayes, A., Kelly, S.P., & O'Connell, R.G. (2018). Reconciling age-related changes in behavioural and neural indices of human perceptual decision-making. *Nature Human Behaviour, 2,* 955-966.

Michalareas, G., Vezoli, J., van Pelt, S., Schoffelen, J.M., Kennedy, H., & Fries, P. (2016) Alpha-beta and gamma rhythms subserve feedback and feedforward influences among human visual cortical areas. *Neuron, 89,* 384-397.

Müller-Gethmann, H., Ulrich, R., & Rinkenauer, G. (2003). Locus of the effect of temporal preparation: Evidence from the lateralized readiness potential. *Psychophysiology, 40,* 597–611.

Niemi, P. & Näätänen, R. (1981). Foreperiod and simple reaction time. *Psychological Bulletin, 89,* 133-162.

Nieuwenhuis, S., Jepma, M., & Wagenmakers, E.-J. (2012). Temporal expectation may affect the onset, not the rate, of evidence accumulation [electronic response to Rohenkohl, Cravo, Wyart, & Nobre (2012). Temporal expectation improves the quality of sensory information. *Journal of Neuroscience, 32,* 8424-8428]

Nobre, A.C., Correa, A., & Coull, J.T. (2007). The hazards of time. *Current Opinion in Neurobiology, 17,* 465-470.

Nobre, A.C., & van Ede, F. (2018). Anticipated moments: temporal structure in attention. *Nature Reviews Neuroscience, 19,* 34-48.

Nunez, M.D., Gosai, A., Vandekerckhove, J., & Srinivasan, R. (2019). The latency of a visual evoked potential tracks the onset of decision making. *Neuroimage, 197,* 93-108.

O'Connell, R.G., Shadlen, M.N., Wong-Lin, K., & Kelly, S.P. (2018). Bridging neural and computational viewpoints on perceptual decision-making. *Trends in Neuroscience, 41,* 838-852.

Palmer, J., Huk, A.C., & Shadlen, M.N. (2005). The effect of stimulus strength on the speed and accuracy of a perceptual decision. *Journal of Vision, 5,* 376–404.

Praamstra, P., Kourtis, D., Kwok, H.F., & Oostenveld, R. (2006). Neurophysiology of implicit timing in serial choice reaction-time performance. *Journal of Neuroscience, 26,* 5448-5455.

Ratcliff, R. (2002). A diffusion model account of response time and accuracy in a brightness discrimination task: fitting real data and failing to fit fake but plausible data. *Psychonomic Bulletin & Review, 9,* 278-291.

Ratcliff, R., Smith, P.L., Brown, S.D., & McKoon, G. (2016). Diffusion decision model: Current issues and history. *Trends in Cognitive Sciences, 20,* 260-281.

Rohenkohl, G., Cravo, A.M., Wyart, V., & Nobre, A.C. (2012a). Temporal expectation improves the quality of sensory information. *Journal of Neuroscience, 32,* 8424-8428.

Rohenkohl, G., Cravo, A.M., Wyart, V., & Nobre, A.C. (2012b). Re: Temporal expectation may affect the onset, not the rate, of evidence accumulation [electronic response to Nieuwenhuis, S., Jepma, M., & Wagenmakers, E.-J. Temporal expectation may affect the onset, not the rate, of evidence accumulation. *Journal of Neuroscience, 32,* 8424-8428]

Rohenkohl, G. & Nobre, A.C. (2011). α oscillations related to anticipatory attention follow temporal expectations. *Journal of Neuroscience, 31,* 14076-14084.

Rolke, B., & Hofmann, P. (2007). Temporal uncertainty degrades perceptual processing. *Psychonomic Bulletin and Review, 14,* 522-526.

Samaha, J., Bauer, P., Cimaroli, S., & Postle, B.R. (2015). Top-down control of the phase of alpha-band oscillations as a mechanism for temporal prediction. *Proceedings of the National Academy of Sciences, 112,* 8439-8444.

Schroeder, C.E., & Lakatos, P. (2009). Low-frequency neuronal oscillations as instruments of sensory selection. *Trends in Neurosciences, 1,* 9-18.

Seibold, V. C., Bausenhart, K. M., Rolke, B., & Ulrich, R. (2011). Does temporal preparation increase the rate of sensory information accumulation? *Acta Psychologica, 137,* 56-64.

Shalev, N., Nobre, A.C., & van Ede, F. (2019). Time for what? Breaking down temporal anticipation. Trends in Neurosciences,.42, 373-374.

Smith, P.L. & Ratcliff, R. (2009). An integrated theory of attention and decision making in visual signal detection. *Psychological Review, 116,* 283-317.

Spiegelhalter, D.J., Best, N.G., Carlin, B.P., & van der Linde, A. (2002). Bayesian measures of model complexity and fit. *Journal of the Royal Statistical Society: Series B, 64,* 583–639.

Spieser, L., Kohl, C., Forster, B., Bestmann, S., & Yarrow, K. (2018). Neurodynamic evidence supports a forced-excursion model of decision-making under speed/accuracy instructions. *eNeuro, 5,* e0159.

Stefanics, G., Hangya, B., Hernádi, I., Winkler, I., Lakatos, P., & Ulbert, I. (2010). Phase entrainment of human delta oscillations can mediate the effects of expectation on reaction speed. *Journal of Neuroscience, 30,* 13578-13585.

Tandonnet, C., Burle, B., Vidal, F., & Hasbroucq, T. (2006). Knowing when to respond and the efficiency of the cortical motor command: A Laplacian ERP study. *Brain Research, 1109,* 158–163.

Thut, G., Nietzel, A., Brandt, S.A., & Pascual-Leone, A. (2006). Alpha-band electroencephalographic activity over occipital cortex indexes visuospatial attention bias and predicts visual target detection. *Journal of Neuroscience, 26,* 9494-9502.

Urai, A.E., & Pfeffer, T. (2014). An action-independent signature of perceptual choice in the human brain. *Journal of Neuroscience, 34,* 5081-5082.

Vandekerckhove, J., Tuerlinckx, F., & Lee, M.D. (2011). Hierarchical diffusion models for two-choice response times. *Psychological Methods, 16,* 44–62.

van den Brink, R.L. Wynn, S., & Nieuwenhuis, S. (2014). Post-error slowing as a consequence of disturbed low-frequency oscillatory phase entrainment. *Journal of Neuroscience, 34,* 11096-11105.

van Diepen, R.M., Cohen, M.X., Denys, D., & Mazaheri, A. (2015). Attention and temporal expectations modulate power, not phase, of ongoing alpha oscillations. *Journal of Cognitive Neuroscience, 27,* 1573-1586.

van Dijk, H., Schoffelen, J.M., Oostenveld, R., & Jensen, O. (2008). Prestimulus oscillatory activity in the alpha band predicts visual discrimination ability. *Journal of Neuroscience, 28,* 1816-1823.

van Kerkoerle, T., Selfa, M.W., Dagninoa, B., Gariel-Mathisa, M-A., Poorta, J., van der Togta, .C, Roelfsemaa, P.R. (2014). Alpha and gamma oscillations characterize feedback and feedforward processing in monkey visual cortex. *PNAS, 111,* 14332–14341.

Vangkilde, S., Coull, J.T., & Bundesen, C. (2012). Great expectations: temporal expectation modulates perceptual processing speed. *Journal of Experimental Psychology: Human Perception and Performance, 38,* 1183-1191.

van Vugt, M.K., Beulen, M.A., & Taatgen, N.A. (2019). Relation between centro-parietal positivity and diffusion model parameters in both perceptual and memory-based decision making. *Brain Research, 1715,* 1-12.

Wetzels, R., & Wagenmakers, E.J. (2012) A default Bayesian hypothesis test for correlations and partial correlations. *Psychonomic Bulletin & Review, 19,* 1057-1064.

Wiecki, T.V., Sofer, I., & Frank, M.J. (2013). HDDM: Hierarchical Bayesian estimation of the drift-diffusion model in Python. *Frontiers in Neuroinformatics, 7,* 14.

Zhang, J., Rittman, T., Nombela, C., Fois, A., Coyle-Gilchrist, I., Barker, R.A., Hughes, L.E., & Rowe, J.B. (2016). Different decision deficits impair response inhibition in progressive supranuclear palsy and Parkinson's disease. *Brain, 139,* 161-173.